

Phonon-like and single particle dynamics in liquid lithium

T. Scopigno¹, U. Balucani², A. Cunsolo³, C. Masciovecchio³, G. Ruocco⁴, F. Sette³, R. Verbeni³¹ Università di Trento and Istituto Nazionale di Fisica della Materia, I-38100, Trento, Italy.² Istituto di Elettronica Quantistica, Consiglio Nazionale delle Ricerche, I-50127, Firenze, Italy.³ European Synchrotron Radiation Facility, B.P. 220 F-38043 Grenoble, Cedex France.⁴ Università di L'Aquila and Istituto Nazionale di Fisica della Materia, I-67100, L'Aquila, Italy.
(August 26, 2021)

The dynamic structure factor, $S(Q;E)$, of liquid lithium ($T=475$ K) has been determined by inelastic x-ray scattering (IXS) in the momentum transfer region ($Q = 1.4 - 110 \text{ nm}^{-1}$). These data allow to observe how, in a simple liquid, a phonon-like collective mode evolves towards the single particle dynamics. As a function of Q , one finds: i) at low Q 's, a sound mode with a positive dispersion of the sound velocity, ii) at intermediate Q 's, excitations whose energy oscillates similarly to phonons in the crystal Brillouin zones, and iii) at high Q 's, the $S(Q;E)$ approaches a Gaussian shape, indicating that the single particle dynamics has been reached.

PACS numbers: 61.25.Mv, 61.10.Eq, 61.20.Ne

The spectrum of density fluctuations, $S(Q;E)$, of a liquid shows a very rich phenomenology with features strongly dependent on the considered momentum, Q , and energy, E , regions [1,2]. The shape of the $S(Q;E)$ is well established in the small and high Q limits. In the hydrodynamics limit, i.e. at $Q=Q_M \ll 1$ (Q_M is the position of the first maximum of the static structure factor $S(Q)$), the spectrum shows three peaks – the Brillouin triplet. They are respectively the Stokes and AntiStokes propagating compressional modes – dispersing linearly with the adiabatic sound velocity v_s , and the thermal diffusion mode centered at zero energy transfer. In the opposite limit, i.e. at $Q=Q_M \gg 1$, one reaches the so called impulse approximation, where the excited particles acquires a kinetic energy much higher than any inter-particle potential energy. Therefore the target particle behaves as a free particle, and the $S(Q;E)$ lineshape reflects the particles' initial state momentum distribution. Considering the Boltzmann distribution, the $S(Q;E)$ reduces to a Gaussian centered at the recoil energy $\hbar^2 Q^2 = 2M$, and with variance $\hbar^2 K_B T Q^2 = M$. Here, M is the particle mass. The evolution between these two limit cases is affected by a realm of dynamical processes as the interaction of sound waves with other degrees of freedom (translational diffusion, rotations and internal modes for molecules), and the interaction between different collective modes, responsible, for example, for the slowing down of the diffusional dynamics in supercooled liquids. Moreover, when Q is comparable to Q_M , important modifications of the Brillouin triplet occur also as a consequence of structural effects. In fact, the sound waves in the liquid cannot be longer described as density fluctuation of a continuum medium, and the local structure with its intrinsic disorder becomes relevant. Compared to the crystalline case, the absence of long range order will prevent to a certain extent, in the liquid, the replication of the sound dispersion relation in high order Brillouin Zones (BZ).

This rich phenomenology has motivated, since long

time, the experimental study of the dynamics of liquid systems. Using ultrasound absorption methods and Brillouin light scattering techniques, the sound waves, and their interactions with the relaxation processes active in the liquid, have been studied in great detail up to $Q=Q_M \sim 10^{-3}$. Similarly, Inelastic Neutron Scattering (INS) has been used at very large Q transfers to determine the $S(Q;E)$ in the impulse approximation, and in Q regions close to Q_M to determine the $S(Q;E)$ lineshape when the two limit description are expected to fail [3,4]. The kinematic limitations on the accessible $Q-E$ region of existing INS instruments [5] did not allow to study with continuity and under comparable experimental conditions the liquid dynamics in the Q range spanning from the collective to the single particle behaviors. Moreover the neutron scattering cross-section accounts for two different contributions: besides the coherent cross section – probing the collective dynamics – there is an incoherent contribution which, at each wavevector, reflects the single particle motion and therefore hides the crossover between the previously quoted regimes. The development of Inelastic X-ray Scattering (IXS) [6] has allowed, recently, to sensibly extend the accessible $Q-E$ region in disordered materials and to avoid the incoherent contribution.

In this work we report the determination by IXS of the dynamic structure factor of liquid lithium in the $1.4 - 110 \text{ nm}^{-1}$ Q range, corresponding to $Q=Q_M \sim 5 \cdot 10^2$. Lithium has been chosen because, among the simple monoatomic liquids, is the one that is best suited to IXS. Indeed, its low mass gives recoil energies observable in the considered Q -range, and its low atomic number and large sound velocity ($\sim 5000 \text{ m/s}$) give optimal signal with the available energy resolution, compensating for the large form factor decrease at high Q values [7]. The $S(Q;E)$ spectra, reported to their absolute scale exploiting the zeroth and first moments sum rules, show the transition from a triplet to a Gaussian. The maxima, $\langle Q \rangle$, of the longitudinal current spectra ($E^2 = Q^2 S(Q;E)$) show an almost linear dispersion relation at low Q – typical

of a sound wave – and a completely different dependence in the high Q limit, where it approaches the parabolic dispersion of the free particle. These two regions are joined by oscillations of $S(Q)$, which are in phase with the structural correlations, as observed in the $S(Q)$. Finally, in the low Q region these data confirm the existence of positive dispersion of the sound velocity.

The experiment has been carried out at the very high energy resolution IXS beam line ID 16, at the European Synchrotron Radiation Facility. The incident x-ray beam is obtained by a back-scattering monochromator operating at the Si(h h h) ($h=7, 9, 11$) reflections [8]. The scattered photons are collected by spherical silicon crystal analyzers, operating at the same Si(h h h) reflection [9]. The total energy resolution obtained from the measurement of $S(Q_M; E)$ in a Plexiglas sample which is dominated by elastic scattering is 8.5 meV full-width-half-maximum for $h=7$, 3 meV for $h=9$ and 1.5 meV for $h=11$. The momentum transfer, $Q = 2k_h \sin(\theta_s/2)$, with k_h the wavevector of the incident photon and θ_s the scattering angle, is selected either between 1.4 and 25 nm⁻¹ by rotating a 7 m long analyser arm in the horizontal scattering plane (data taken at $h=9$ and 11), or between 24 and 110 nm⁻¹ by rotating a 3 m long analyser arm in the vertical scattering plane ($h=7$). The total Q resolution has been set to 0.4 nm⁻¹ at $h=9$ and 11, and 1 nm⁻¹ at $h=7$. On the horizontal arm, five independent analyzers were used to collect simultaneously five different Q values, determined by the constant angular offset of 1.5° between neighbour analyzers. The vertical arm houses only one analyzer. Energy scans are done by varying the temperature of the monochromator with respect to that of the analyzer crystals. The absolute energy calibration between successive scans is better than 1 meV. Each scan took about 180 min, and each Q -point spectrum has been obtained from the average of 2 to 8 scans depending on h and the Q -transfer. The data have been normalized to the intensity of the incident beam. The liquid lithium uncapped container is made out of austenitic stainless steel with a resistance heater, used to keep the liquid at $T = 475$ K. The 20 mm long sample, kept together by surface tension, was maintained in a 10⁻⁶ bar vacuum. The lithium has been loaded in an argon glove box. In the $Q-E$ region of interest, empty vacuum chamber measurements gave either the flat electronic detector background of 0.6 counts/min or, at $9 < Q < 13$ nm⁻¹, a small elastic line due to scattering from the chamber kapton windows (each 50 mm thick) which was subtracted from the data.

The IXS spectra of liquid lithium are reported in Fig. 1 at the indicated Q transfer values. The low Q data show the Brillouin triplet structure with the energy of the inelastic peaks increasing with Q up to a Q value of 12 nm⁻¹. This value corresponds to $Q_M=2$, as deduced from the $S(Q)$ reported in Fig. 2. One can interpret, therefore, the dispersion up to $Q_M=2$ as that of the longitudinal

acoustic branch in the pseudo-first BZ. Furthermore, similarly to what it is found in the second BZ of a crystal, we observe that, also in liquid lithium, the energy of the acoustic modes decreases with increasing Q from $Q_M=2$ to Q_M . Increasing Q above Q_M , i.e. in the "third" or higher BZs, one finds that the spectrum gets increasingly broader and distinct peaks are no longer observable. At the highest Q -values one finds that the $S(Q; E)$ becomes a symmetric peak centered at energies larger than $E = 0$. Beside the observation of dispersion in a first and second pseudo-BZs, it is also important to note that the broadening of the excitations monotonically increase with Q to the extent that towards the end of the second pseudo-BZ the inelastic features are no longer showing a well defined peak.

The previous qualitative description can be made substantially more quantitative considering that the dynamic structure factor $S(Q; E)$ can be derived from the measured intensity, $I(Q; E)$, using the zeroth and first moment sum rules for $S(Q; E)$:

$$m_{(0)}^S = \int_{-\infty}^{\infty} S(Q; E) dE = S(Q); \quad (1)$$

$$m_{(1)}^S = \int_{-\infty}^{\infty} E S(Q; E) dE = \hbar^2 Q^2 = 2M. \quad (2)$$

Considering that $I(Q; E) = \int_{-\infty}^{\infty} dE^0 S(Q; E^0) R(E - E^0)$, where $R(E)$ is the experimental resolution function and $\langle Q \rangle$ is a factor taking into account the scattering geometries – efficiencies and the lithium atomic form factor, the first moments of the experimental data, $m_{(0)}^I$ and $m_{(1)}^I$, and those of the resolution function, $m_{(0)}^R$ and $m_{(1)}^R$, are related to $m_{(0)}^S$ and $m_{(1)}^S$ by:

$$m_{(0)}^I = \langle Q \rangle m_{(0)}^S m_{(0)}^R; \quad (3)$$

$$m_{(1)}^I = \langle Q \rangle (m_{(0)}^S m_{(1)}^R + m_{(1)}^S m_{(0)}^R); \quad (4)$$

From the previous equation one derives that

$$S(Q) = \frac{\hbar^2 Q^2}{2M} (m_{(1)}^I / m_{(0)}^I - m_{(1)}^R / m_{(0)}^R)^{-1}; \quad (5)$$

This procedure has been utilised to put the $S(Q; E)$ on an absolute scale using the experimentally determined $I(Q; E)$ and $R(E)$. The reliability of this procedure is shown in Fig. 2 where we obtain an excellent agreement between the $S(Q)$ values obtained by Eq. 4 and those derived by Molecular Dynamics (MD) simulation [10].

The possibility to express $S(Q; E)$ in absolute units allows to compare the IXS data with the Gaussian lineshape expected for the $S(Q; E)$ when the single particle limit is reached. This comparison is reported in Fig. 1b, where each solid line represents the sum of two Gaussians:

$$G(Q; E) = \frac{1}{2} \sum_{i=6,7}^X \frac{C_i}{\sigma_i} \exp(-(E - E_i)^2 / 2\sigma_i^2) \quad (6)$$

where $C_6 = 0.08$ and $C_7 = 0.92$ are the natural abundances of the ^6Li and ^7Li isotopes, $E_i = \hbar^2 Q^2 / 2M_i$ their recoil energies and $\frac{2}{i} = \hbar^2 K_B T Q^2 / M_i$. The progressively better agreement between the data and $G(Q; E)$ with increasing Q testifies the evolution towards the single particle behaviour, which seems to be reasonably well reached at the highest investigated Q values and at the considered temperature.

The dispersion relation of the energy (Q) of the inelastic signal observed in Fig. 1 is obtained by determining the maximum of the current spectra. This allows us to estimate (Q) independently from any specific model for the $S(Q; E)$. Examples of current spectra, obtained from the spectra in Fig. 1, are shown in Fig. 3. The values of (Q) have been determined by a parabolic fit of the maximum region in the Stokes side. The values of (Q) are reported in Fig. 4. In Fig. 4a are also reported the linear dispersion of the adiabatic sound velocity (dotted line) and the parabolic dispersion expected for the single particle dynamics. We observe that (Q) is close to the adiabatic sound mode at the lowest Q values, and it shows a positive dispersion before reaching the maximum of the first pseudo-BZ. This is emphasized in Fig. 4b, where the low Q region is expanded, and the inset reports directly the sound velocity $v(Q) = (Q)/Q$. This behaviour confirms previous MD [11-13] and experimental [14] data in a similar Q region on lithium and other alkali liquid metals. With increasing Q values, the points in Fig. 4a show not only a second pseudo-BZ, as already pointed out in Fig. 1, but also a series of oscillations that dump out with increasing Q - here, (Q) approaches the single particle line. These oscillations are in anti-phase with the oscillations found in the $S(Q)$ (see Fig. 2) and can, therefore, be associated to the local order in the liquid. It is of great interest to be able to follow all the way from the sound mode to the free particle regime the evolution of (Q) . Beside the importance of a unified picture in such a wide Q region these data provide the workbench for a quantitative theoretical analysis of the shape of the $S(Q; E)$.

In conclusion, using IXS, we have been able to measure the collective dynamics in a simple liquid from the collective modes regime, dominated by sound-like excitations, all the way towards the impulse approximation regime, dominated by single particle dynamics. This textbook result provides a picture on how in a simple liquid the structural correlations induce important deviation from the "continuum" picture used in the hydrodynamic limit, and gives effects qualitatively similar to those as the BZs in crystals.

We acknowledge valuable help of H. Mueller from the Chemistry Laboratory at ESRF for his technical assistance during the sample manipulation.

- [1] J.P. Boon and S. Yip, "Molecular Hydrodynamics" (McGraw-Hill, New York, 1980).
- [2] U. Balucani, M. Zoppi, "Dynamics of the liquid state", Clarendon Press, Oxford (1994).
- [3] P.H.K. De Jong, Ph.D. thesis, Technische Universiteit Delft, Netherlands (1993).
- [4] P.H.K. De Jong, P. Verkerk and L.A. De Graaf, J. Non Cryst. Solids, 156-8, 48 (1993).
- [5] S.W. Lovesey, "Theory of neutron scattering from condensed matter", Clarendon Press, Oxford (pag. 120), (1994).
- [6] E. Burkel, 1991, "Inelastic Scattering of X-rays with very high Energy Resolution", Springer Verlag, Berlin.
- [7] "Handbook of Thermodynamic and Transport Properties of Alkali Metals", (Osheta et al.) Blackwell Scientific Publications, pag. 735 (1985).
- [8] R. Verbeni, F. Sette, M. Krish, U. Bergmann, B. Gorges, C. Halaboussis, K. Martel, C. Masciovecchio, J.F. Ribois, G. Ruocco and H. Sinn, J. of Synchrotron Radiation, 3, 62 (1996).
- [9] C. Masciovecchio, U. Bergmann, M. Krish, G. Ruocco, F. Sette, R. Verbeni, Nucl. Inst. and Meth., B-111, 181 and B-117, 339 (1986).
- [10] T. Scopigno et al., to be published.
- [11] A. Rahman, Phys. Rev. Lett. 32, 52 (1974);
- [12] T. Bodensteiner, C. Morke, W. G. Laser, B. Dömer, Phys. Rev. A 45, 5709 (1992).
- [13] A. Torcini, U. Balucani, P.H.K. de Jong and P. Verkerk, Phys. Rev. E 51, 3126 (1995).
- [14] H. Sinn et al., Phys. Rev. Lett. 78, 1715 (1997).

FIGURE CAPTIONS

FIG. 1 - Dynamic Structure Factor (Density Correlation Function) of Lithium at $T = 475\text{K}$ measured by IXS and normalized according to the procedure discussed in the text. The spectra on the left column are taken with a resolution $E = 3\text{ meV}$ using Si (999) reflection; Those on the right column with $E = 8.5\text{ meV}$ using the Si (777) reflection. In the latter column the comparison with a gaussian lineshape (full line) expected in the free particle limit is also reported.

FIG. 2 - Test of normalization accuracy: the $S(Q)$ values as extracted from IXS normalization (open symbols) are reported together with computer simulation data (full line) [10]. The inset shows an enlargement of the small Q region and the dotted line is the $Q \rightarrow 0$ limit expected from the isothermal sound velocity.

FIG. 3 - Current Correlation Function $J(Q; E)$ obtained from the $S(Q; E)$ spectra reported in Fig. 1 as $J(Q; E) = E^2 Q^2 S(Q; E)$.

FIG. 4 - Sound dispersion of Lithium. Fig. 4a - The energy position of the Stokes Peak of the Current Correlation Function (open circles) are reported together with the dispersion expected in two limiting cases: low Q linear dispersion with hydrodynamic velocity (dotted line) and high Q (full line) parabolic dispersion of the impulse approximation. These two dispersion curves have been computed assuming the presence of both ^6Li and ^7Li in their natural abundances (see text and Eq. 6).

Fig. 4b - Detail of the 'small Q ' (below the First Sharp Diffraction Peak) region. The deviation of the acoustic sound velocity from the adiabatic value (dotted line) at increasing wavevectors is observed (positive dispersion).

This figure "Lifig1.jpg" is available in "jpg" format from:

<http://arxiv.org/ps/cond-mat/9911021v1>

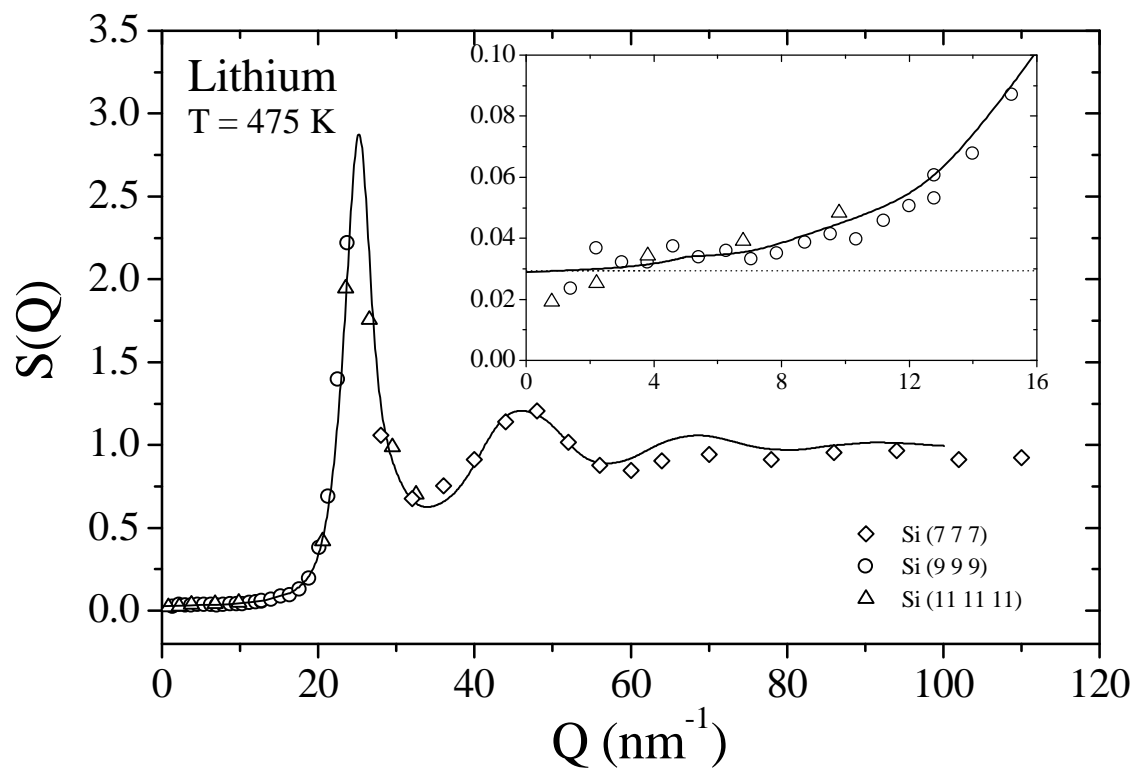


Fig. 2 - T. Scopigno et al.

This figure "Lifig3.jpg" is available in "jpg" format from:

<http://arxiv.org/ps/cond-mat/9911021v1>

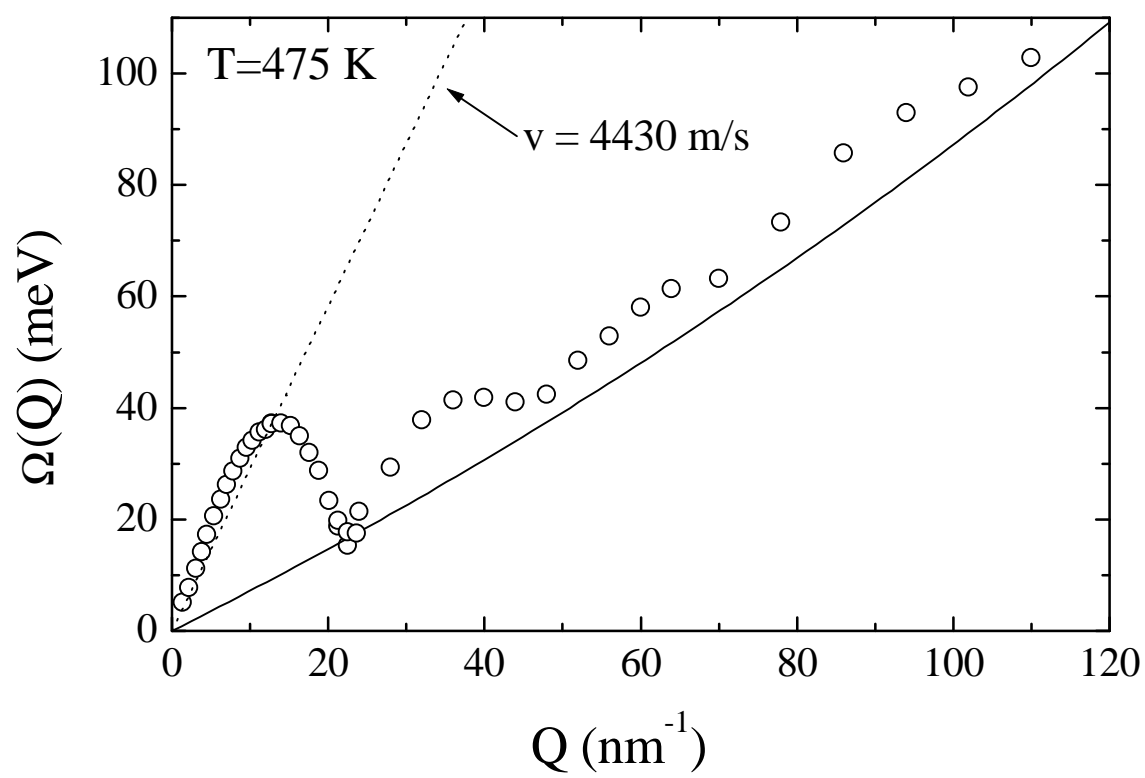


Fig. 4a - T. Scopigno et al.

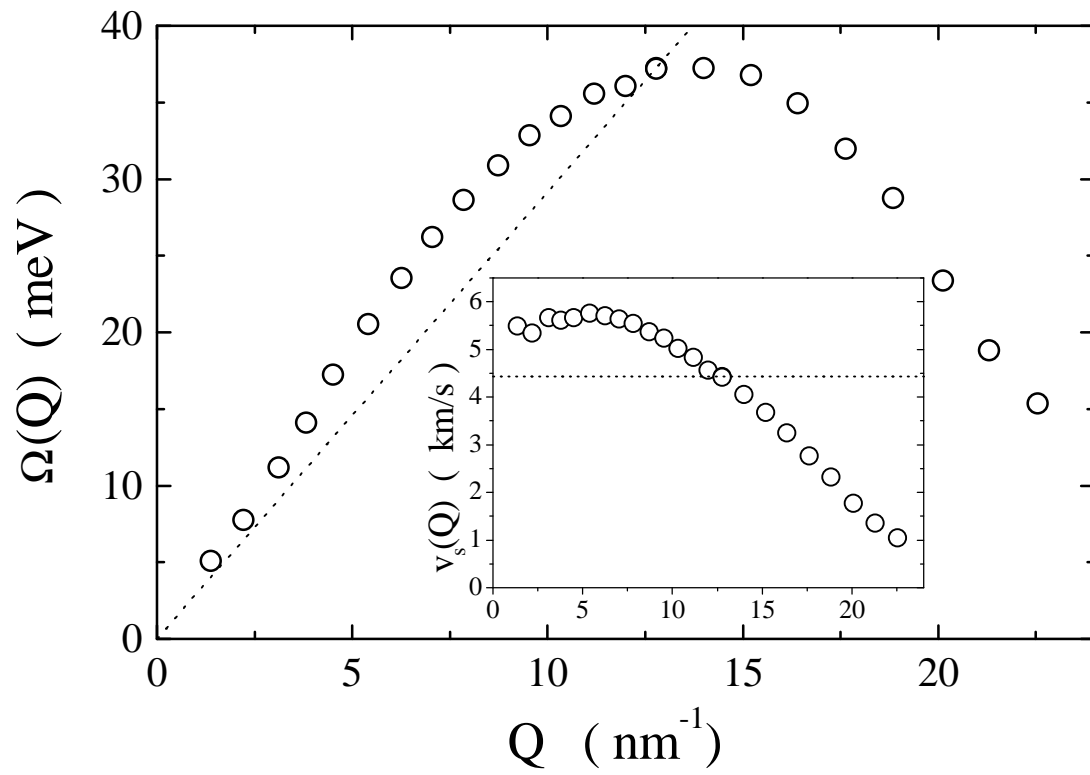


Fig. 4b - T. Scopigno et al.